

See discussions, stats, and author profiles for this publication at: <https://www.researchgate.net/publication/273886331>

Wavelet q -Fisher Information for Scale-Invariant Network Traffic

Chapter · January 2013

DOI: 10.1201/b14574-14

CITATIONS

0

READS

29

4 authors, including:



Julio Ramirez-Pacheco

Center for Research and Advanced Studies of the National Polytechnic Institute

46 PUBLICATIONS 98 CITATIONS

SEE PROFILE



Homero Toral-Cruz

University of Quintana Roo

40 PUBLICATIONS 119 CITATIONS

SEE PROFILE



Pablo Velarde Alvarado

Universidad Autónoma de Nayarit

27 PUBLICATIONS 43 CITATIONS

SEE PROFILE

Some of the authors of this publication are also working on these related projects:



Impacto fiscal y financiero frente a la globalización [View project](#)



Modelos y algoritmos basados en entropía para la detección y prevención de intrusiones de red [View project](#)

Chapter 10

Wavelet q -Fisher Information for Scale-Invariant Network Traffic

Julio Ramírez-Pacheco, Deni Torres-Román,
Homero Toral-Cruz, and Pablo Velarde-Alvarado

Contents

10.1 Introduction.....	265
10.2 Wavelet Analysis of Scaling Processes.....	267
10.2.1 Scaling Processes.....	267
10.2.2 Wavelet Analysis of Scaling Signals.....	269
10.3 Wavelet q -Fisher Information of $1/f^\alpha$ Signals	270
10.3.1 Time-Domain Fisher's Information Measure.....	270
10.3.2 Wavelet q -Fisher Information	271
10.3.3 Applications of Wavelet FIM	275
10.4 Level-Shift Detection Using Wavelet q -Fisher Information.....	275
10.4.1 Problem of Level-Shift Detection	275
10.4.2 Level-Shift Detection Using Wavelet q -Fisher Information	276
10.5 Results and Discussion.....	276
10.5.1 Application to Variable Bit Rate Video Traces	278
10.6 Conclusions.....	279
References	279

10.1 Introduction

The study of the properties of computer network traffic is important for many aspects of computer network design, performance evaluation, network simulation, capacity planning, and network algorithmic design, among others. In the very beginning of computer network traffic modeling,

the traffic itself was considered Markovian because older telephone network traffic was suitably described by this model; thus, it was unsurprising to consider the characteristics of network traffic similar to those of the telephone network. Markovian models permitted straightforward computations of performance issues due to its being short-range dependent (SRD); moreover, because of the ease of computation and lack of memory, they became very popular. The modeling of computer network traffic with Markovian models ended when Leland et al. [1], based on detailed studies of high-resolution network measurements, discovered that network traffic did not follow the Markovian model but instead is more appropriately modeled by self-similar or fractal stochastic processes. Subsequent studies not only validated this finding but also found self-similar features in additional network configurations [2,3]. The self-similar nature of network traffic indicated that computer network traffic behaves “statistically” similar at different scales of observation. In fact, persistence behavior was observed in local area network traffic at small as well as high levels of observation. This finding was contrary to commonly observed features of Markovian models where, for large scale, the traffic appeared to reduce to white noise. The self-similar nature of network traffic implied that numerous results based on the Markovian model needed to be thoroughly revised. Later, many authors reported that, when considering traffic as a self-similar process, many Internet quality of service (QoS) metrics such as delay, packet-loss rate, and jitter increased. Because of this, it was obvious that a characterization of the traffic flowing through a network was necessary; based on the observed characteristics, actions specifically designed to maintain the QoS of the network under acceptable levels were required. The characterization of traffic was in principle performed by estimating the parameters that determine its behavior. The Hurst parameter (or the self-similarity parameter) provided a complete characterization of self-similar processes; however, due to the complex characteristics of observed traffic, nowadays, it is clear that complementary techniques are required [4–6]. Self-similar processes are related to long-memory, fractal, and multifractal processes, and it is common to find in the scientific literature claims that traffic is self-similar, fractal, or multifractal. Self-similar processes along with long-memory, fractal, $1/f$, and multifractal processes belong to the class of scaling or scale-invariant signals. The theory of scaling signals has been relevant for the study of many phenomena occurring in diverse fields of science and technology. Some aspects of physiology such as heart rate variability [7] are suitably modeled by scaling signals, and the parameter of scaling signals determines much of the properties of the heart and the individual under study [7]. Electroencephalogram (EEG) signals obtained in humans and animals are also appropriately described by scaling signals [8], but they also model the traffic flowing through computer communications [2,9,10], the turbulence in physics, the noise observed in electronic devices [11], and the time series obtained in economy [3] and finance, among others. Many techniques and methodologies have been proposed to analyze these processes [12–14]; however, they have shown to be limited for the rich set of complexities observed in the data [5,15]. In addition, many articles have concluded that no single technique of analysis is sufficient for providing efficient and robust estimation of the scaling parameter [12]. Because of this, current works concentrate in developing cutting-edge techniques that are robust to trends, level-shifts, and missing values embedded in the data under study. The presence of these phenomenologies significantly impacts the estimation process and can lead to misinterpretation of the phenomena [7,12]. In this context, recent results that attempt to study the complexities of the underlying process using wavelet-based entropies provide interesting alternatives. In fact, it has been demonstrated, for example, that wavelet Tsallis q -entropies behave as a sum-cosh window [6] and that this behavior can be used to detect multiple mean level shifts embedded in the scaling signal under study and for the classification of scaling signals as stationary or nonstationary as well [15]. This chapter presents novel techniques based on wavelet information tools for the important

References have been renumbered. Please check for changes throughout.

problem of detecting level shifts embedded in scaling signals. This problem has been recognized as of sufficient importance because it impacts the estimation of the scaling parameter α [16,17]. The chapter therefore defines the concept of wavelet q -Fisher information and provides a thorough study of its properties for scaling signal analysis. Information planes that attempt to describe the complexities of scaling signals are constructed for these processes. In fact, this chapter shows that wavelet q -Fisher information provides plausible explanations of the complexities associated to scaling signals; based on this, level-shift detection capabilities can be attached to it. Extensive experimental studies validate the theoretical findings and allow one to study the effect of the parameter q on wavelet Fisher's information's behavior and the level-shift detection capabilities within scaling signals. The parameter q allows further flexibility and can be adapted to the characteristics of the data under study. In the limit of $q \rightarrow 1$, it reduces to the standard wavelet Fisher information as defined in the work of Ramírez-Pacheco et al. [18].

The rest of the chapter is organized as follows: In Section 10.2, the properties and definitions of scaling signals are studied with sufficient detail, and their wavelet analysis is explored. Also, some important results are reviewed for fractional Brownian motion (fBm), fractional Gaussian noise (fGn), and discrete pure power-law (PPL) signals. Section 10.3 derives the wavelet q -Fisher information for scaling signals and studies its properties. In this section, generalizations of the wavelet q -Fisher information are presented in terms of the q -analysis. Section 10.4 details the level-shift detection problem and presents some results in which the wavelet q -Fisher information is applied for this problem. Section 10.6 draws the conclusions of the chapter.

10.2 Wavelet Analysis of Scaling Processes

10.2.1 Scaling Processes

Scaling processes of parameter α , also called $1/f^\alpha$ or power-law processes, have been extensively applied and studied in the scientific literature because they model diverse phenomena [9,10] within these fields. These processes are sufficiently characterized by the parameter α , called the scaling index, which determines many of their properties. Various definitions have been proposed in the scientific literature; some are based on their characteristics such as self-similarity or long memory, and others are based on the behavior of their power spectral density (PSD). In this section, a scaling process is a random process for which the associated PSD behaves as a power-law in a range of frequencies [2,19], that is,

$$S(f) \sim c_f |f|^{-\alpha}, f \in (f_a, f_b) \quad (10.1)$$

where c_f is a constant, $\alpha \in R$ is the scaling index, and f_a, f_b represent the lower and upper bound frequencies on which the power-law scaling holds. Depending on f_a, f_b and α , several particular scaling processes and behaviors can be identified. Independently of α , local regularity and band-pass power-law behavior is observed whenever $f_a \rightarrow \infty$ and $f_a > f_b \gg 0$, respectively. When the scaling index α is taken into consideration, long-memory behavior is observed when both $0 < \alpha < 1$ and $f_a > f_b \rightarrow 0$. Self-similar features (in terms of distributional invariance under dilations) are observed in all the scaling index range for all f . Scaling index α determines not only the stationary and nonstationary conditions of the scaling process but also the smoothness of their sample path realizations. The greater the scaling index α , the smoother their sample paths. In fact, as long as $\alpha \in (-1, 1)$, the scaling process is stationary [or stationary with long memory for small f and $\alpha \in (0, 1)$] and nonstationary

when $\alpha \in (1,3)$. Some transformations can make a stationary process appear nonstationary and vice versa. Outside the range $\alpha \in (-1,3)$, several other processes can be identified; for example, the so-called extended fBm and fGn defined in the work of Serinaldi [12] provide generalizations to the standard fBm and fGn signals. The persistence of scaling processes can also be quantified by the index α , and within this framework, scaling processes possess negative persistence as long as $\alpha < 0$, positive weak long persistence when $0 < \alpha < 1$, and positive strong long persistence whenever $\alpha > 1$. Scaling signals encompass a large family of well-known random signals, such as fBm and fGn [20], PPL processes [19], and multifractal processes [2]. fBm, $B_H(t)$, comprises a family of Gaussian, self-similar processes with stationary increments; because of the Gaussianity, it is completely characterized by its autocovariance sequence (ACVS), which is given by

$$\mathbb{E}B_H(t)B_H(s) = R_{BH} = \frac{\sigma^2}{2} \left\{ |t|^{2H} + |s|^{2H} - |t-s|^{2H} \right\}, \quad (10.2)$$

where $0 < H < 1$ is the Hurst index. fBm is nonstationary, and as such, no spectrum can be defined on it; however, fBm possesses an average spectrum of the form $S_{fBm}(f) \sim c|f|^{-(2H+1)}$ as $f \rightarrow 0$, which implies that $\alpha = 2H + 1$ [21]. fBm has been applied very often in the literature; however, it is its related process, fGn, that has gained widespread prominence because of the stationarity of its realizations. fGn, $G_{H,\delta}(t)$, obtained by sampling an fBm process and computing increments of the form $G_{H,\delta}(t) = 1/\delta \{B_H(t+\delta) - B_H(t), \delta \in Z_+\}$ (i.e., by differentiating fBm), is a well-known Gaussian process. The ACVS of this process is given by

$$\mathbb{E}G_{H,\delta}(t)G_{H,\delta}(t+\tau) = \frac{\sigma^2}{2} \left\{ |\tau+\delta|^{2H} + |\tau-\delta|^{2H} - 2|\tau|^{2H} \right\} \quad (10.3)$$

where $H \in (0,1)$ is the Hurst index. The associated PSD of fGn is given by [19]

$$S_{fGn}(f) = 4\sigma_x^2 C_H \sin^2(\pi f) \sum_{j=-\infty}^{\infty} \frac{1}{|f+j|^{2H+1}} \quad |f| \leq \frac{1}{2}, \quad (10.4)$$

where σ_x is the process variance and C_H is a constant. fGn is stationary and, for large enough τ and under the restriction of $1/2 < H < 1$ possesses long-memory or long-range dependence (LRD). The scaling index α associated to fGn signals is given by $\alpha = 2H - 1$ as its PSD, given by Equation 10.4, behaves asymptotically as $S_{fGn}(f) \sim c|f|^{-(2H+1)}$ for $f \rightarrow 0$. Another scaling process of interest is the family of discrete PPL processes, which are defined as processes for which their PSD behaves as $S_x(f) = C_x |f|^{-\alpha}$ for $|f| \leq 1$, where $\alpha \in \mathbb{R}$ and C_x represents a constant. PPL signals are stationary when the power-law parameter $\alpha < 1$ and nonstationary whenever $\alpha > 1$. As stated in the work of Percival [19], the characteristics of these processes and those of fBm/fGn are similar; however, the differences between fBm and PPLs with $\alpha > 1$ are more evident. In fact, differentiation of stationarity/nonstationarity is far more difficult for PPL than for fBm/fGn. Figure 10.1 displays some realizations of fGn, fBm, and PPL processes. The scaling index α of the PPL signals are identical to the scaling index of the associated fGn and fBm. Note that the characteristics of the sample paths of fGn are fairly different from those of fBm. In the case of PPL processes, this differentiation is not so evident; in fact, when the scaling indexes approach the boundary $\alpha = 1$, classification

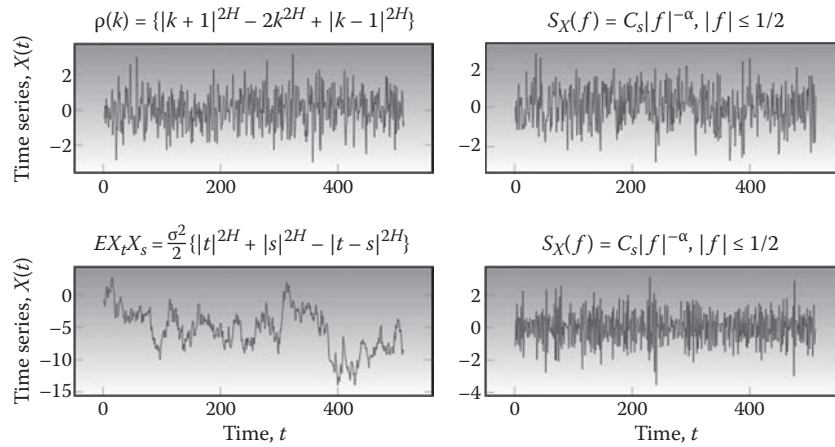


Figure 10.1 Sample path realizations of some scaling processes. (Top left) fGn with $\alpha = -0.1$; (top right) PPL process with $\alpha = -0.1$; (bottom left) fBm signal with $\alpha = 1.9$; (bottom right) PPL process with $\alpha = 1.9$.

becomes complex. For further information on the properties, estimators, and analysis techniques of scaling processes, please refer to references [2,9,10,12,13,19,22].

10.2.2 Wavelet Analysis of Scaling Signals

Wavelets and wavelet transforms have been applied for the analysis of deterministic and random signals in almost every field of science [5,23,24]. The advantages of wavelet analysis over standard techniques of signal analysis have been widely reported, and its potential for nonstationary signal analysis is proven. Wavelet analysis represents a signal X_t in the time-scale domain by the use of an analyzing or mother wavelet, $\psi_o(t)$ [25]. For our purposes, $\psi_o(t) \in L_1 \cap L_2$ and the family of shifted and dilated $\psi_o(t)$ form an orthonormal basis of $L_2(\mathbb{R})$. In addition, the finiteness of the mean average energy $\left(\mathbb{E} \int |X(u)|^2 du < \infty \right)$ on the scaling process allows one to represent it as a linear combination of the form

$$X_t = \sum_{j=1}^L \sum_{k=-\infty}^{\infty} d_x(j, k) \psi_{j,k}(t), \tag{10.5}$$

where $d_x(j, k)$ represents the discrete wavelet transform (DWT) of X_t , and $\{\psi_{j,k}(t) = 2^{-j/2} \psi_o(2^{-j}t - k), j, k \in \mathbb{Z}\}$ is a family of dilated (of order j) and shifted (of order k) versions of $\psi_o(t)$. The coefficients $d_x(j, k)$ in Equation 10.5, obtained by DWT, represent a random process for every j and a random variable for fixed j and k , and as such, many statistical analyses can be performed on them. Equation 10.5 represents signal X_t as a linear combination of L detail signals, obtained by means of the DWT. DWT is related to the theory of multiresolution signal representation, in which signals (or processes) can be represented at different resolutions based on the number of detail signals added to the low-frequency approximation signal. Detail random signals ($d_x(j, k)$) are obtained by projections of signal X_t into wavelet spaces W_j , and approximation

Table 10.1 Wavelet Spectrum or Wavelet Variance Associated to Different Types of Scaling Processes

Type of Scaling Process	Associated Wavelet Spectrum or Variance
Long-memory process	$\mathbb{E}d_X^2(j, k) \sim 2^{j\alpha} C(\psi, \alpha), \quad C(\psi, \alpha) = c_\gamma \int f ^{-\alpha} \Psi(f) ^2 df$
Self-similar process	$\mathbb{E}d_X^2(j, k) = 2^{j(2H+1)} \mathbb{E}d_X^2(0, k)$
Hsssi process	$\text{Vard}_X^2(j, k) = 2^{j(2H+1)} \text{Vard}_X(0, 0)$
Discrete PPL process	$\mathbb{E}d_X^2(j, k) = C 2^{j\alpha}$

Note: $\mathbb{E}(\cdot)$, $\text{Var}(\cdot)$, and $\psi(\cdot)$ represent expectation, variance, and Fourier integral operators, respectively.

coefficients $(a_x(j, k))$ are obtained by projections of X_t into related approximation spaces V_j . In the study of scaling processes, wavelet analysis has been primarily applied in the estimation of the wavelet variance [4,5]. Wavelet variance or spectrum of a random process accounts for computing variances of wavelet coefficients at each scale. Wavelet variance not only has permitted to propose estimation procedures for the scaling index α but also to compute entropies associated to the scaling signals. Wavelet spectrum has also been used for detecting nonstationarities embedded in Internet traffic [5]. For stationary zero-mean processes, wavelet spectrum is given by

$$\mathbb{E}d_X^2(j, k) = \int_{-\infty}^{\infty} S_X(2^{-j} f) |\Psi(f)|^2 df, \tag{10.6}$$

where $\Psi(f) = \int \psi(t) e^{-j2\pi ft} dt$ is the Fourier integral of $\psi_o(t)$ and $S_X(\cdot)$ represents the PSD of X_t . Table 10.1 summarizes the wavelet spectrum for some standard scaling processes. For further details on the analysis, estimation, and synthesis of scaling processes, please refer to the works of Abry and Veitch [25] and Bardet [26] and references therein.

10.3 Wavelet q -Fisher Information of $1/f^\alpha$ Signals

10.3.1 Time-Domain Fisher’s Information Measure

Fisher’s information measure (FIM) has recently been applied in the analysis and processing of complex signals [27–29]. In the work of Martin et al. [27], FIM was applied to detect epileptic seizures in EEG signals recorded in human and turtles; later, Martin et al. [28] reported that FIM can be used to detect dynamical changes in many nonlinear models such as the logistic map and Lorenz model, among others. The work of Telesca et al. [29] reported on the application of FIM for the analysis of geoelectrical signals. Recently, Fisher information has been extensively applied in quantum mechanical systems for the study of single particle systems [30] and also in the context of atomic and molecular systems [31]. FIM has also been used in combination with Shannon entropy power to construct the so-called Fisher–Shannon information plane/product (FSIP) [32]. The FSIP was recognized in that work to be a plausible method for nonstationary signal analysis. Let X_t be a signal with associated probability density $f_X(x)$. Fisher’s information (in time domain) of signal X_t is defined as

$$I_X = \int \left(\frac{\partial}{\partial_x} f_X(x) \right)^2 \frac{dx}{f_X(x)}. \quad (10.7)$$

Fisher's information I_X is a nonnegative quantity that yields large (possibly infinite) values for smooth signals and small values for random disordered data. Accordingly, Fisher's information is large for narrow probability densities and small for wide (flat) ones [33]. Fisher information is also a measure of the oscillatory degree of a waveform; highly oscillatory functions have large Fisher information [30]. Fisher's information has mostly been applied in the context of stationary signals using a discretized version of Equation 10.7:

$$I_X = \sum_{k=1}^L \left\{ \frac{(p_{k+1} - p_k)^2}{p_k} \right\}, \quad (10.8)$$

for some probability mass function (pmf) $\{p_k\}_{k=0}^L$. Equation 10.8 can be computed in sliding windows resembling a real-time computation. In this case, Fisher's information is often called FIM. Generalizations of Fisher's information have been defined in the literature. In fact, Plastino et al. [8] defined the q -Fisher information of a pmf as

$$I_q = \sum_j \{p_{j+1} - p_j\}^2 p_j^{q-2}. \quad (10.9)$$

The parameter q provides further analysis flexibility and can highlight nonstationarities embedded in the signal under study. In this context, q -Fisher information is again a descriptor of the complexities associated to random signals and can attain high values.

10.3.2 Wavelet q -Fisher Information

This section defines a generalized version of Fisher information in the wavelet domain, derives a closed-form expression for this quantifier, and explores the possibility of using wavelet Fisher information for the analysis of scaling signals. Let $\{X_t, t \in \mathbb{R}\}$ be a real-valued scaling process satisfying Equation 10.1, with DWT $\{d_X(j, k), (j, k) \in \mathbb{Z}^2\}$ and associated wavelet spectrum $\mathbb{E}|d_X(j, k)|^2 \sim c_X 2^{j\alpha}$ (c_X is a constant and \mathbb{E} is the expectation operator) [5]. A pmf obtained from the wavelet spectrum of scaling signals is given by the expression [6]

$$p_j \equiv \frac{1/N_j \sum_k \mathbb{E} d_X^2(j, k)}{\sum_{i=1}^M \left\{ 1/N_i \sum_k \mathbb{E} d_X^2(j, k) \right\}} = 2^{(j-1)\alpha} \frac{1 - 2^\alpha}{1 - 2^{\alpha M}}, \quad (10.10)$$

where N_j (N_i) represents the number of wavelet coefficients at scale j (i), $M = \log_2(N)$ with $N \in \mathbb{Z}_+$ the length of the data, and $j = 1, 2, \dots, M$. Substituting Equation 10.10 into Equation 10.9 results in the wavelet q -Fisher information of a scaling signal, which is given by

$$\begin{aligned}
 I_q &= (1 - 2^\alpha)^2 \left\{ \frac{1 - 2^\alpha}{1 - 2^{\alpha M}} \right\}^q \left\{ \frac{1 - 2^{\alpha q(M-1)}}{1 - 2^{\alpha q}} \right\} \\
 &= 2^{\alpha \left(1 - \frac{q}{2}\right) + 2} \left\{ \sinh_{1-v_1}^2(u_2) \right\} \left\{ \frac{\sinh_{1-\frac{v_2}{M-1}}^q(u_2)}{\sinh_{1-v_1}(u_1)} \right\}
 \end{aligned} \tag{10.11}$$

$$\times \left\{ \frac{\sinh_{1-v_1}(u_1)}{\sinh_{1-v_2}^q(u_2)} \right\} \left\{ \frac{P_{\text{num}}}{P_{\text{den}}} \right\}, \tag{10.12}$$

where P_{num} and P_{den} are given by the following polynomial expressions:

$$\begin{aligned}
 P_{\text{num}} &= 2 \cosh_{1-\frac{v_1}{(M-2)}}(u_1(M-2)) + 2 \cosh_{1-\frac{v_1}{(M-4)}}(u_1(M-4)) \\
 &\quad + 2 \cosh_{1-\frac{v_1}{(M-6)}}(u_1(M-6)) + \dots
 \end{aligned} \tag{10.13}$$

$$\begin{aligned}
 P_{\text{den}} &= 2 \cosh_{1-\frac{v_2}{(M-1)}}(u_2(M-1)) + 2 \cosh_{1-\frac{v_2}{(M-3)}}(u_2(M-3)) \\
 &\quad + 2 \cosh_{1-\frac{v_2}{(M-5)}}(u_2(M-5)) + \dots
 \end{aligned} \tag{10.14}$$

with $u_1 = \alpha q \ln_q(2)/2$, $u_2 = qu_1$, $v_1 = 2(1-q)/(\alpha q)$, and $v_2 = qv_1$. Equations 10.12 through 10.18 involve the use of the q -analysis [34], where $\sinh_q(x) \equiv \{e_q^x - e_q^{\ominus_q x}\}/2$ and $\cosh_q(x) \equiv \{e_q^x + e_q^{\ominus_q x}\}/2$ denote the q -sinh and q -cosh functions, respectively. $e_q^x \equiv \{1 + (1-q)x\}^{1/(1-q)}$ and $\ominus_q x \equiv (-x)/\{1 + (1-q)x\}$ denote the q -exponential and q -difference functions, respectively. Equation 10.12 allows one to relate the results of wavelet q -Fisher information with the ones of the standard wavelet FIM. In fact, in the $q \rightarrow 1$ limiting case, wavelet q -Fisher information turns out to be the standard wavelet Fisher information for which the following holds:

$$I_1 = \frac{(2^\alpha - 1)^2 (1 - 2^{\alpha(M-1)})}{1 - 2^{\alpha M}} \tag{10.15}$$

$$= 2^{\frac{\alpha}{2} + 2} \sinh^2\left(\frac{\alpha \ln 2}{2}\right) \left\{ \frac{P_{\text{num}}^M(2 \cosh(\alpha \ln 2/2))}{P_{\text{den}}^{M+1}(2 \cosh(\alpha \ln 2/2))} \right\}, \tag{10.16}$$

where $P_{\text{num}}^M(\cdot)$ and $P_{\text{den}}^{M+1}(\cdot)$ denote polynomials of argument $2 \cosh(\alpha \ln 2/2)$ that are given by

$$P_{\text{num}}^M(\cdot) = (2 \cosh u)^M - \frac{2(M-3)}{2!} 2 \cosh u^{M-2} + \frac{3(M-4)(M-5)}{3!} (2 \cosh u)^{M-5} - \dots \tag{10.17}$$

$$P_{\text{den}}^{M+1}(\cdot) = (2 \cosh u)^{M+1} - \frac{(M-2)}{1!} 2 \cosh u^{M-1} + \frac{(M-3)(M-4)}{2!} (2 \cosh u)^{M-3} - \dots \tag{10.18}$$

where $u = \alpha \ln 2/2$. An interesting question is how the behavior of wavelet q -Fisher information is affected by q . To answer this question, Figure 10.2 displays the wavelet q -Fisher information for $q \in (0,1)$. Note that, as q approaches 1, wavelet q -Fisher information attains higher values for nonstationary signals ($\alpha > 1$). Therefore, if the signal is smooth or has a narrow probability density, then it is more likely to have a large wavelet q -Fisher value. Note also that, as long as $q \in (0,1)$, the form of the Fisher information is similar to that of the standard wavelet Fisher information [18] (high for highly oscillatory data and low for smooth signals). For the case where $q \in (0,1)$, wavelet q -Fisher has a behavior that is similar to that of the top left plot of Figure 10.3. In fact, when $q = 2$, wavelet q -Fisher information is symmetric with respect to $\alpha = 0$. Wavelet q -Fisher information reverses its behavior as long as $q > 2$, that is, in this case, highly oscillatory functions or functions with narrow probability densities display low values of their Fisher information, whereas smooth and flat probability densities display high values. Unlike the case $q > 1$, the $q > 2$ case decreases the range of variation of the wavelet q -Fisher information; thus, the detection of nonstationarities

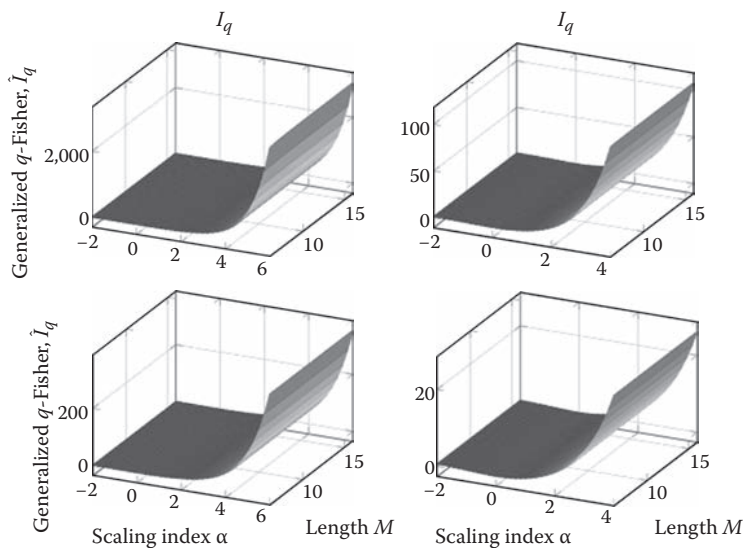


Figure 10.2 Wavelet q -Fisher information for $1/f^\alpha$ signals. (Top left) Fisher information with $q = 0.2$; (top right) $q = 0.4$; (bottom left) Fisher information for $q = 0.6$; (bottom right) $q = 0.8$.

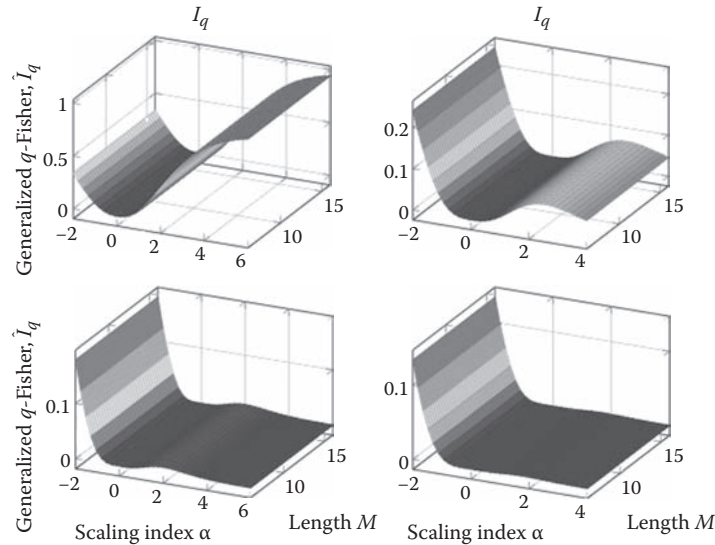


Figure 10.3 Wavelet q -Fisher information for $1/f^\alpha$ signals. (Top left) Fisher information with $q = 2.5$; (top right) $q = 3$; (bottom left) Fisher information for $q = 3.5$; (bottom right) $q = 4$.

embedded in a signal is more difficult. Based on this behavior of the wavelet q -Fisher information, it is clear that values of $q \in (0,1)$ are suitable for detecting nonstationarities embedded in the data.

In this case, the value of the q -Fisher information is significantly higher for nonstationary signals. Figure 10.4 presents the theoretical wavelet q -Fisher information for scaling signals with $\alpha \in (-4,4)$ and fixed-length $M = 16$. According to Figure 10.4, for $q < 1$, wavelet q -Fisher information is high for nonstationary signals ($\alpha \geq 1$) and low for stationary ones ($\alpha < 1$). Fisher information

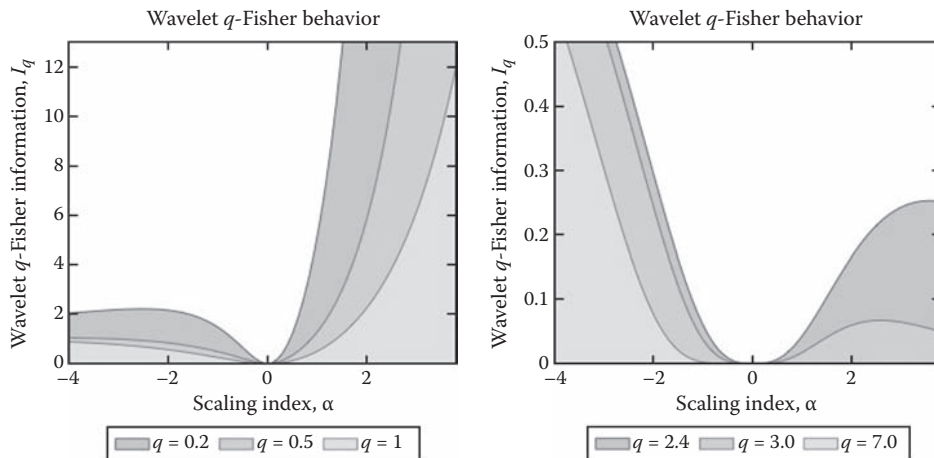


Figure 10.4 Wavelet q -Fisher information of scaling signals. Wavelet q -Fisher information is exponentially increasing (or decreasing) for signals with $\alpha > 0$ (or $-\infty < \alpha < 0$) and minimum for scaling signals with $\alpha = 0$.

consequently is high for correlated scaling signals and low for anticorrelated ones [18]. Fisher information is minimum ($I_q = 0$) for completely random signals ($\alpha = 0$).

10.3.3 Applications of Wavelet FIM

Because wavelet q -Fisher information describes properly the characteristics and complexities of fractal $1/f^\alpha$ signals, many applications can be identified using this complexity-based framework. In fact, based on the fact that wavelet q -Fisher information achieves large values for nonstationary signals and small values for stationary ones (for the case $q \in (0,1)$), a potential application area of wavelet q -Fisher information is in the classification of fractal signals as fractional noises and motions. Classification of $1/f^\alpha$ signals as motions or noises remains as an important, attractive, and unresolved problem in scaling signal analysis [7,35,36] because the nature of the signal governs the selection of estimators, the shape of quantifiers such as q th-order moments, and the nature of correlation functions [37]. Another important potential application of wavelet q -Fisher information, related to the classification of signals, is in the blind estimation of scaling parameters [38]. Blind estimation refers to estimating α independently of signal type (stationary or nonstationary). Wavelet q -Fisher information can also be utilized for the detection of structural breaks in the mean embedded in $1/f^\alpha$ signals. Structural breaks in the mean affect significantly the estimation of scaling parameters leading to biased estimates of α and consequently in misinterpretation of the phenomena. In fact, in the work of Stoev et al. [5], it was demonstrated that the well-known Abry–Veitch estimator overestimates the scaling index α in the presence of a single level shift leading to values of $H = (\alpha + 1)/2 > 1$, which, in principle, is not permissible in theory. In the following, the section concentrates on the detection of structural breaks in the mean embedded in synthesized stationary fGn signals by the use of wavelet q -Fisher information. The section studies anticorrelated and correlated versions of fGn and the power of wavelet q -Fisher information in detecting single structural breaks in the mean in these signals.

10.4 Level-Shift Detection Using Wavelet q -Fisher Information

10.4.1 Problem of Level-Shift Detection

Detection and location of structural breaks in the mean (level shifts) have been recognized as an important research problem in many areas of science and engineering [16,17]. In the Internet traffic analysis framework, detection, location, and mitigation of level shifts significantly improve on the estimation process. In fact, the presence of a single level shift embedded in a stationary fGn results in an estimated $H > 1$ [5]. This, in turn, results in misinterpretation of the phenomena under study and also in inadequate construction of q th-order moments. Let $B(t), t \in \mathbb{R}$, be a $1/f$ signal with level shifts at time instants $\{t_1, t_{1+L}, \dots, t_j, t_{j+L}\}$. $B(t)$ can be represented as

$$B(t) = X(t) + \sum_{j=1}^J \mu_j 1_{[t_j, t_{j+L}]}(t), \quad (10.19)$$

where $X(t)$ is a signal satisfying Equation 10.1 and $\mu_j 1_{[a,b]}(t)$ represents the indicator function of amplitude μ_j in the interval $[a,b]$. The problem of level-shift detection reduces to identify the

points $\{t_j, t_{j+L}\}_{j \in J}$, where a change in behavior occurs. Often, the change is perceptible by eye, but frequently, this is not the case and alternative quantitative methods are preferred. In what follows, a description of the procedure for detecting level shifts in $1/f$ signals by wavelet q -Fisher information is described; later, results on simulated fGn signals are presented.

10.4.2 Level-Shift Detection Using Wavelet q -Fisher Information

To detect the presence of level shifts in fractal $1/f$ signals, wavelet q -Fisher information is computed in sliding windows. A window of length w , located in the interval $m\Delta \leq t_k < m\Delta + w$ applied to signal $\{X(t_k), k = 1, 2, \dots, N\}$, is

$$X(m; w, \Delta) = X(t_k) \prod \left(\frac{t - m\Delta}{w} - \frac{1}{2} \right) \quad (10.20)$$

where $m = 0, 1, 2, \dots, m_{\max}$, Δ is the sliding factor, and $\Pi(\cdot)$ is the well-known rectangular function. Note that Equation 10.20 represents a subset of $X(t_k)$; thus, by varying m from 0 to m_{\max} and computing wavelet q -Fisher information on every window, the temporal evolution of wavelet FIM is followed. Suppose the wavelet q -Fisher information at time m (for sliding factor Δ) is denoted as $I_x(m)$. Then a plot of the points

$$\left\{ (w + m\Delta, I_x(m)) \right\}_{m=0}^{m_{\max}} := I_X \quad (10.21)$$

represents such time evolution. In the work of Stoev et al. [5], it was demonstrated that the presence of a sudden jump in a stationary fractal signal will cause the estimated $\hat{H} > 1$. The level shift thus causes the signal under observation become nonstationary. In the wavelet q -Fisher information framework, this sudden jump will cause its value to increase suddenly [according to its studied behavior for $q \in (0, 1)$]. Therefore, a sudden jump increase in the plot of Equation 10.21 can be considered as an indicator of the occurrence of a single level shift in the signal. These theoretical findings are experimentally tested by the use of synthesized scaling signal with level shifts. The synthesized signals correspond to fGn signals generated using the circular embedding algorithm [39,40] (also known as the Davies and Harte algorithm).

10.5 Results and Discussion

Figure 10.5 displays the level-shift detection capabilities of wavelet q -Fisher information for a correlated fGn signal with Hurst exponent $H = 0.7$ and a single structural break located at $t_b = 8192$. The length of the signal is $N = 2^{14}$ points with the break located in the middle and amplitude $\sqrt{\sigma_X^2}$, where σ_X^2 is the fGn variance. The top plot displays the signal and also the level shift (in white) added to its structure for illustration purposes only. It is important to note that the amplitude of the considered and studied level shifts are weak; however, wavelet q -Fisher information detects appropriately its location. The presence of a single level shift embedded in the fGn signal is therefore detected by a sudden increase (in the form of an impulse) in the wavelet q -Fisher information value when computed in sliding windows.

In Figure 10.5, wavelet q -Fisher information was computed with $q = 0.6$. The Hurst exponent $H = 0.7$ means that the signal under study is stationary with LRD. Figure 10.6 displays the level-shift detection capabilities of wavelet q -Fisher information when considering anticorrelated fGn signals. Anticorrelated signals have the property that high values are likely to be followed by low values and vice versa. Note that, for these types of signals, wavelet q -Fisher information effectively detects and also locates level shift embedded in the signal structure. Therefore, independently of the type of anticorrelated fGn signal ($H < 0.5$), wavelet q -Fisher information appropriately detects weak level shift with amplitudes higher than $\sqrt{\sigma_X^2}/2$. The analysis performed in Figure 10.6 was performed in sliding windows of length $W = 2^{11}$ at steps of $\Delta = 90$.

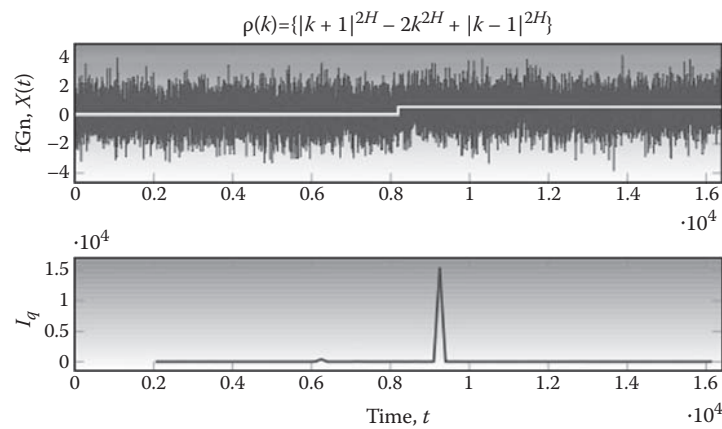


Figure 10.5 Detection of a single structural break at $t_b = 8192$ embedded in an fGn signal with parameter $H = 0.7$.

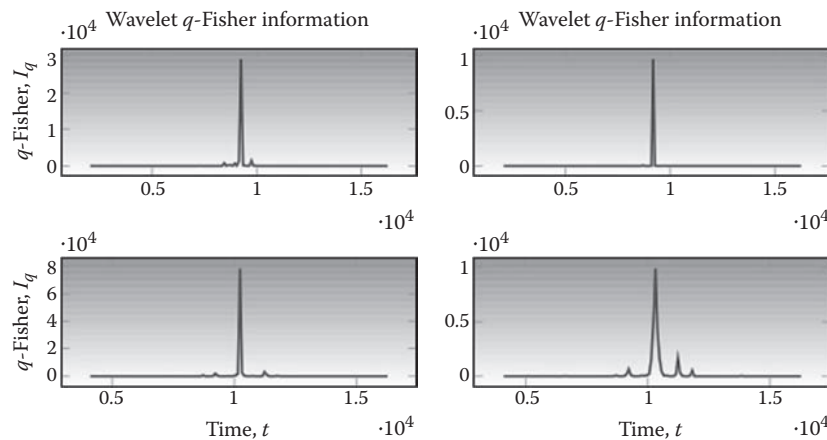


Figure 10.6 Wavelet q -Fisher information for anticorrelated fGn signals. (Top left) wavelet q -Fisher information for an fGn signal with $H = 0.1$; (top right) $H = 0.2$; (bottom left) $H = 0.3$; (bottom right) $H = 0.4$. The amplitude of the level shifts was set to $\sqrt{\sigma_X^2}/2$.

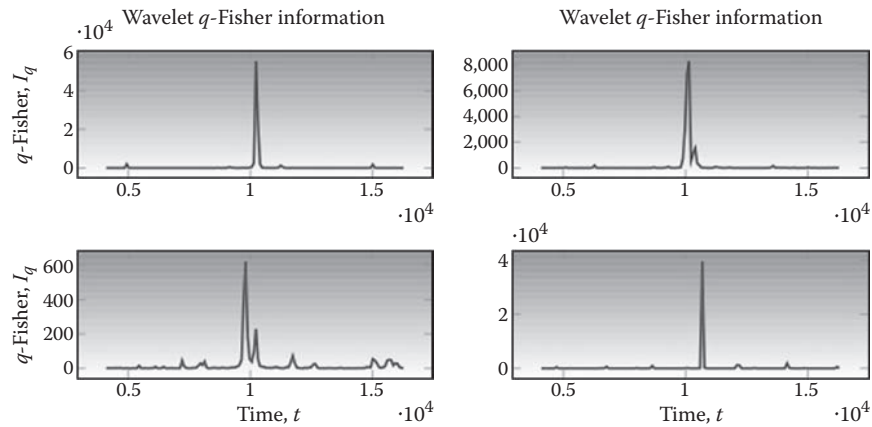


Figure 10.7 Wavelet q -Fisher information for Gaussian white noise and correlated fGn signals. (Top left) wavelet q -Fisher information for a Gaussian white noise signal ($H = 0.5$); (top right) an fGn signal with $H = 0.6$; (bottom left) an fGn signal with $H = 0.8$; (bottom right) an fGn with $H = 0.9$. The amplitude of the level shifts was set to $\sqrt{\sigma_x^2/2}$.

The parameter q of Fisher was set to $q = 0.6$, and the length of the considered signal was $N = 2^{14}$ points. Similar results were obtained when increasing $q \rightarrow 1$. In fact, by increasing the amplitudes of the level shifts, better detection capabilities can be observed in wavelet q -Fisher information; however, a higher level shift can also be detected by eye. Figure 10.7 presents the level-shift detection capabilities of wavelet q -Fisher information for correlated fGn signals with long-memory and Gaussian white noise. The top left plot displays the wavelet q -Fisher information for a totally disordered Gaussian white noise signal ($H = 0.5$). Note that wavelet q -Fisher information effectively detects the level shift within this signal. For correlated signals, wavelet q -Fisher information performs well and appropriately detects the presence of the level shifts.

Note, however, that, in some cases, wavelet q -Fisher information values decrease in amplitude but are sufficiently high to be considered as level shifts. Based on these results, wavelet q -Fisher information therefore detects appropriately level shifts embedded in stationary fGn signals. The detection is accomplished independently of the range of the Hurst parameter and in consequence of the correlation structure in the signal. Wavelet q -Fisher information therefore provides an interesting alternative to the problem of level-shift detection in fGn signals.

Please check orphan section head 10.5.1.

10.5.1 Application to Variable Bit Rate Video Traces

Variable bit rate (VBR) video is expected to account for a large amount of the traffic flowing through next-generation converged networks. The study of the properties of VBR video traffic is therefore important because novel algorithms can be designed to the characteristics observed within this traffic. VBR video traffic is long-range dependent and the long-memory parameter is in many cases $H > 1$, which, in theory, is not permissible. The $H > 1$ case suggests that the VBR video traffic may be subjected to level shifts or nonstationarities embedded within the signal. In this context, we apply the wavelet q -Fisher information to a large set of VBR video traces and found that many traces display many impulse-shaped peaks in their wavelet q -Fisher information. Figure 10.8 displays the wavelet q -Fisher information for an H.263 encoded video signal. Note that this VBR video signal presents many impulse-shaped peaks, which indicate the presence of

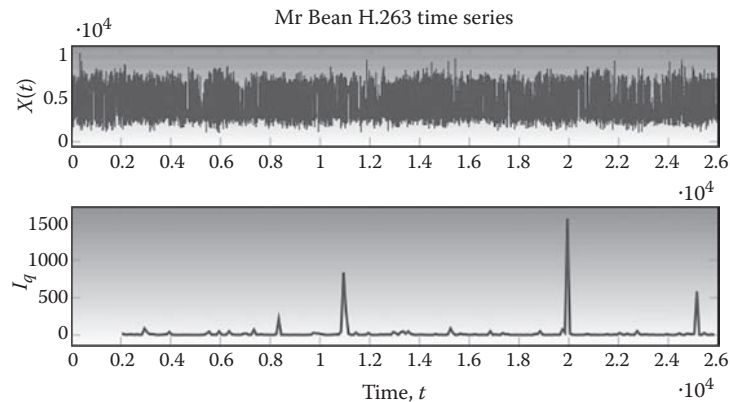


Figure 10.8 Wavelet q -Fisher information for an H.263 encoded video signal. (Top) time series (frame size) in bits of Mr. Bean movie; (bottom) corresponding wavelet q -Fisher information of Mr. Bean movie with $q = 0.8$.

level shifts embedded within the VBR video signal. This result also explains why wavelet-based estimator displays long-memory index estimation of $H > 1$.

10.6 Conclusions

In this chapter, the notion of wavelet q -Fisher information was introduced. A closed-form expression for this quantifier was developed for scaling signals, and its properties and behavior, in a range of the parameter α and for various q , were studied. It was demonstrated through experimental studies with simulated fGn signals that wavelet q -Fisher information not only provides appropriate descriptions of the complexities of these signals but also allows one to detect structural breaks in the mean embedded in their structure. In fact, wavelet q -Fisher information allows to effectively and timely detect structural breaks embedded in anticorrelated and correlated fGn signals.

References

1. Leland, W. E., Taqqu, M. S., Willinger, W., and Wilson, D. V.: 'On the self-similar nature of Ethernet traffic (extended version)', *IEEE/ACM Transactions on Networking*, 1994, **2**, (1), pp. 1–15.
2. Lee, I. W. C., and Fapojuwo, A. O.: 'Stochastic processes for computer network traffic modelling', *Computer Communication*, 2005, **29**, pp. 1–23.
3. Beran, J.: 'Statistical methods for data with long-range dependence', *Statistical Science*, 1992, **7**, pp. 404–416.
4. Shen, H., Zhu, Z., and Lee, T. M. C.: 'Robust estimation of the self-similarity parameter in network traffic using wavelet transform', *Signal Processing*, 2007, **87**, (9), pp. 2111–2124.
5. Stoev, S., Taqqu, M. S., Park, C., and Marron, J. S.: 'On the wavelet spectrum diagnostic for Hurst parameter estimation in the analysis of Internet traffic', *Computer Networks*, 2005, **48**, (3), pp. 423–445.
6. Ramírez-Pacheco, J., and Torres-Román, D.: 'Cosh window behaviour of wavelet Tsallis q -entropies in $1/f^\alpha$ signals', *Electronics Letters*, 2011, **47**, (3), pp. 186–187.
7. Eke, A., Hermán, P., Bassingthwaight, J. B., Raymond, G., Percival, D. B., Cannon, M., Balla, I., and Ikrényi, C.: 'Physiological time series: distinguishing fractal noises and motions', *Pflügers Archiv*, 2000, **439**, (4), pp. 403–415.

Please provide the expanded form of this journal title.

Please provide the expanded form of this journal title.

Please check and update the status of this entry (provide volume number and page range, if possible).

Please provide the expanded form of this journal title.

Please provide the expanded form of this journal title.

Please provide the expanded form of this journal title.

8. Plastino, A., Plastino, A. R., and Miller, H. G.: 'Tsallis nonextensive thermostatics and Fisher's information measure', *Phys. A*, 1997, **235**, pp. 557–588.
9. Samorodnitsky, G., and Taqqu, M. S.: *Stable Non-Gaussian Random Processes*, Chapman & Hall, New York, USA, 1994.
10. Beran, J.: *Statistics for Long-Memory Processes*, Chapman & Hall, New York, USA, 1994.
11. Mandal, S., Arfin, S. K., and Sarpeshkar, R.: 'Sub-pHz MOSFET 1/f noise measurements', *Electronics Letters*, 2009, **45**, (1), pp. 81–82.
12. Serinaldi, F.: 'Use and misuse of some Hurst Parameter estimators applied to stationary and nonstationary financial time series', *Phys. A*, 2010, **389**, pp. 2770–2781.
13. Malamud, B. D., and Turcotte, D. L.: 'Self-affine time series: measures of weak and strong persistence', *Journal of Statistical Planning and Inference*, 1999, **80**, (1–2), pp. 173–196.
14. Gallant, J. C., Moore, I. D., Hutchinson, M. F., and Gessler, P.: 'Estimating the fractal dimension of profiles: a comparison of methods', *Mathematical Geology*, 1994, **26**, (4), pp. 455–481.
15. Ramírez Pacheco, J., Torres Román, D., and Toral Cruz, H.: 'Distinguishing stationary/nonstationary scaling processes using wavelet Tsallis q - entropies', *Math. Prob. Eng.*, accepted for publication, 2012.
16. Rea, W., Reale, M., Brown, J., and Oxley, L.: 'Long-memory or shifting means in geophysical time series', *Mathematics and Computers in Simulation*, 2011, **81**, (7), pp. 1441–1453.
17. Cappelli, C., Penny, R. N., Rea, W. S., and Reale, M.: 'Detecting multiple mean breaks at unknown points in official time series', *Mathematics and Computers in Simulation*, 2008, **78**, (2–3), pp. 351–356.
18. Ramírez-Pacheco, J., Torres-Román, D., Rizo-Dominguez, L., Trejo-Sanchez, J., and Manzano-Pinzon, F.: 'Wavelet Fisher's information measure of $1/f^\alpha$ signals', *Entropy*, 2011, **13**, pp. 1648–1663.
19. Percival, D. B.: 'Stochastic models and statistical analysis of clock noise', *Metrologia*, 2003, **40**, (3), pp. S289–S304.
20. Mandelbrot, B. B., and Van Ness, J. W.: 'Fractional Brownian motions, fractional noises and applications', *SIAM Review*, 1968, **10**, pp. 422–437.
21. Flandrin, P.: 'Wavelet analysis and synthesis of fractional Brownian motion', *IEEE Transactions on Information Theory*, 1992, **38**, (2), pp. 910–917.
22. Lowen, S. B., and Teich, M. C.: 'Estimation and simulation of fractal stochastic point processes', *Fractals*, 1995, **3**, (1), pp. 183–210.
23. Hudgins, L., Friehe, C. A., and Mayer, M. E.: 'Wavelet transforms and atmospheric turbulence', *Physical Review Letters*, 1993, **71**, (20), pp. 3279–3282.
24. Cohen, A. and Kovacevic, A. J.: 'Wavelets: the mathematical background', *Proceedings of the IEEE*, 1996, **84**, (4), pp. 514–522.
25. Abry, P., and Veitch, D.: 'Wavelet analysis of long-range dependent traffic', *IEEE Transactions on Information Theory*, 1998, **44**, (1), pp. 2–15.
26. Bardet, J. M.: 'Statistical study of the wavelet analysis of fractional Brownian motion', *IEEE Transactions on Information Theory*, 2002, **48**, (4), pp. 991–999.
27. Martin, M. T., Pennini, E., and Plastino, A.: 'Fisher's information and the analysis of complex signals', *Physical Letters A*, 1999, **256**, pp. 173–180.
28. Martin, M. T., Perez, J., and Plastino, A.: 'Fisher information and non-linear dynamics', *Phys. A*, 2001, **291**, pp. 523–532.
29. Telesca, L., Lapenna, V., and Lovullo, M.: 'Fisher information measure of geoelectrical signals', *Phys. A*, 2005, **351**, pp. 637–644.
30. Romera, E., Sánchez-Moreno, P., and Dehesa, J. S.: 'The Fisher information of single particle systems with central potential', *Chemical Physics Letters*, 2005, **414**, pp. 468–472.
31. Luo, S.: 'Quantum Fisher information and uncertainty relation', *Letters in Mathematical Physics*, 2000, **53**, pp. 243–251.
32. Vignat, C., and Bercher, J. F.: 'Analysis of signals in the Fisher–Shannon information plane', *Physical Letters A*, 2003, **312**, pp. 27–33.
33. Frieden, B. R. and Hughes, R. J.: '1/f noise derived from extremized physical information', *Phys. Rev. E*, 49, 1994, 2644–2649.
34. Borges, E. P.: 'A possible deformed algebra and calculus inspired in nonextensive thermostatics', *Phys. A*, 340, 2004, 95–101.

35. Eke, A., Hermán, P., Kocsis, L. and Kozak, L. R., Fractal characterization of complexity in temporal physiological signals, *Physiol. Meas.*, **23**, 2002, R1–38.
36. Deligneres, D., Ramdani, S., Lemoine, L., Torre, K., Fortes, M. and Ninot, G., Fractal analyses of short time series: A re-assessment of classical methods, *J. Math. Psychol.*, **50**, 2006, 525–544.
37. Castiglioni, P., Parato, G., Civijian, A., Quintin, L. and Di Rienzo, M., Local scale exponents of blood pressure and heart rate variability by detrended fluctuation analysis: Effects of posture, exercise and aging, *IEEE Trans. Biomed. Eng.*, **56**, (3), 2009, 675–684.
38. Esposti, F., Ferrario, M. and Signorini, M. G., A blind method for the estimation of the Hurst exponent in time series: Theory and methods, *Chaos*, **18**, (3), 2008, 033126-033126-8.
39. Davies, R. B. and Harte, R. S., Tests for Hurst effect, *Biometrika*, **74**, 1987, 95–101.
40. Cannon, M. J., Percival, D. B., Caccia, D. C., Raymond, G. M. and Bassingthwaight, J. B., Evaluating scaled windowed variance for estimating the Hurst coefficient of time series, *Phys. A*, **241**, 1996, 606–626.

